HUMAN GENE THERAPY 22:935–949 (August 2011)

DOI: 10.1089/hum.2010.121

Research Articles

Recombinant Adeno-Associated Virus-Mediated Gene Transfer for the Potential Therapy of Adenosine Deaminase-Deficient Severe Combined Immune Deficiency

Jared N. Silver,[1] Melissa Elder,[1] Thomas Conlon,[1] Pedro Cruz,[1] Amy J. Wright,[1] Arun Srivastava,[1] and Terence R. Flotte[2]

Abstract

Severe combined immune deficiency due to adenosine deaminase (ADA) deficiency is a rare, potentially fatal pediatric disease, which results from mutations within the *ADA* gene, leading to metabolic abnormalities and ultimately profound immunologic and nonimmunologic defects. In this study, recombinant adeno-associated virus (rAAV) vectors based on serotypes 1 and 9 were used to deliver a secretory version of the *human ADA* (*hADA*) gene to various tissues to promote immune reconstitution following enzyme expression in a mouse model of ADA deficiency. Here, we report that a single-stranded rAAV vector, pTR2-CB-Igκ-hADA, (1) facilitated successful gene delivery to multiple tissues, including heart, skeletal muscle, and kidney, (2) promoted ectopic expression of hADA, and (3) allowed enhanced serum-based enzyme activity over time. Moreover, the rAAV-hADA vector packaged in serotype 9 capsid drove partial, prolonged, and progressive immune reconstitution in ADA-deficient mice.

Overview Summary

Gene therapies for severe combined immune deficiency due to adenosine deaminase (ADA) deficiency (ADA-SCID) over two decades have exclusively involved retroviral vectors targeted to lymphocytes and hematopoietic progenitor cells. These groundbreaking gene therapies represented an unprecedented revolution in clinical medicine but in most cases did not fully correct the immune deficiency and came with the potential risk of insertional mutagenesis. Alternatively, recombinant adeno-associated virus (rAAV) vectors have gained attention as valuable tools for gene transfer, having demonstrated no pathogenicity in humans, minimal immunogenicity, long-term efficacy, ease of administration, and broad tissue tropism (Muzyczka, 1992; Flotte *et al*., 1993; Kessler *et al*., 1996; McCown *et al*., 1996; Lipkowitz *et al*., 1999; Marshall, 2001; Chen *et al*., 2003; Conlon and Flotte, 2004; Griffey *et al*., 2005; Pacak *et al*., 2006; Stone *et al*., 2008; Liu *et al*., 2009; Choi *et al*., 2010). Currently, rAAV vectors are being utilized in phase I/II clinical trials for cystic fibrosis, α-1 antitrypsin deficiency, Canavan's disease, Parkinson's disease, hemophilia, limb–girdle muscular dystrophy, arthritis, Batten's disease, and Leber's congenital amaurosis (Flotte *et al*., 1996, 2004; Kay *et al*., 2000; Aitken *et al*., 2001; Wagner *et al*., 2002; Manno *et al*., 2003; Snyder and Francis, 2005; Maguire *et al*., 2008; Cideciyan *et al*., 2009). In this study, we present preclinical data to support the viability of an rAAV-based gene transfer strategy for cure of ADA-SCID. We report efficient transduction of a variety of postmitotic target tissues *in vivo*, subsequent human ADA (hADA) expression, and enhanced hADA secretion in tissues and blood, with increasing peripheral lymphocyte populations over time.

Introduction

Adenosine deaminase (ADA) is a 41-kDa zinc-dependent enzyme in the purine salvage pathway found ubiquitously in most tissues in predominantly cytosolic and membrane-bound isoforms. ADA deficiency most often manifests as severe combined immune deficiency (SCID) characterized by profound lymphopenia with combined T-, B-, and natural

[1]Department of Pediatrics and Powell Gene Therapy Center, University of Florida College of Medicine, Gainesville, FL 32610.
[2]Department of Pediatrics and Gene Therapy Center, University of Massachusetts Medical School, Worcester, MA 01655.

killer (NK)-cell defects. Children with SCID due to ADA deficiency (ADA-SCID) suffer from life-threatening infections and musculoskeletal, neurologic, pulmonary, renal, and hepatic impairments (Hershfield, 2003; Aiuti, 2004; Cavazzana-Calvo and Fischer, 2007).

The standard of care for ADA-SCID is histocompatible hematopoietic stem cell transplantation, although the availability of human leukocyte antigen–matched sibling or unrelated donors is limited. Numerous patients for whom a histocompatible donor is unavailable receive enzyme replacement therapy with polyethylene glycol–conjugated bovine ADA (PEG-ADA). PEG-ADA provides life-saving, partial immune reconstitution with increased lymphocyte numbers and function via serum-based detoxification of accumulating toxic metabolites, such as adenosine, deoxyadenosine, and deoxy-ATP. However, this therapy is expensive, requires lifetime intramuscular injections, may lead to development of autoimmune phenomena and malignancy, and may decrease in efficacy over time. As a consequence, retroviral gene therapies for correction of ADA-SCID were developed, but most treated patients did not have full correction of their immune defect. Despite a few adverse events reported for ADA-SCID patients treated with retroviral vectors, reports of insertional mutagenesis and subsequent leukemogenesis in patients with X-linked SCID using similar retroviral vectors cast doubt upon safety of retroviral vectors overall. Moreover, although retroviral vectors using enhanced transduction protocols may effectively target dividing cells and possibly hematopoietic stem cells for pronounced and sustained immunological benefit, these vectors do not address nonimmune manifestations of ADA-SCID (Hershfield *et al.*, 1987; Hacein-Bey-Abina *et al.*, 2003; Kohn *et al.*, 2003; Baum *et al.*, 2004; Dave *et al.*, 2004; Lainka *et al.*, 2005; Aiuti *et al.*, 2007; Baum, 2007; Booth *et al.*, 2007; Bushman, 2007; Cavazzana-Calvo and Fischer, 2007; Pike-Overzet *et al.*, 2007).

Recombinant adeno-associated virus (rAAV) vectors are nonpathogenic with relatively low immunogenicity compared with other viral vectors and possess broad tissue tropism and ability to transduce both dividing and nondividing cells. rAAV vectors are capable of long-term persistence within host cells, predominantly as high-molecular-weight episomes (Flotte *et al.*, 1994; Goudy *et al.*, 2001; Song *et al.*, 2004). Such episomal persistence facilitates both long-term transgene expression in postmitotic or slowly dividing target cells and reduced risk of insertional mutagenesis. rAAV serotype 2 vectors not only demonstrate a high degree of transduction efficiency into several cell types *in vitro*, but also efficacy and safety in various small and large animal models *in vivo.* rAAV vectors continue to be pursued as potential therapies for numerous genetic, metabolic, and infectious diseases in phase I/II clinical trials secondary to these characteristics (Flotte *et al.*, 1996, 2004; Duan *et al.*, 1998; Kay *et al.*, 2000; Aitken *et al.*, 2001; Wagner *et al.*, 2002; Manno *et al.*, 2003; Flotte, 2005, 2007; Kapturczak *et al.*, 2005; Snyder and Francis, 2005; Inagaki *et al.*, 2006; Maguire *et al.*, 2008; Cideciyan *et al.*, 2009).

Similarly, rAAV vectors may offer feasible, versatile, safe, and potentially efficacious therapeutic alternatives to hematopoietic stem cell transplantation, PEG-ADA administration, or retroviral gene therapy, for the treatment of ADA-SCID. In the present study, we used a gene therapy strategy to exploit properties of rAAV and rAAV serotypes 1 and 9 (rAAV1 and rAAV9, respectively) similar to the serum-based detoxification observed with administration of PEG-ADA. We designed and cloned an rAAV vector to carry a tagged secretory version of the gene coding for human ADA (hADA), tested this construct in culture for protein expression and secretion, and packaged it in serotype 1 and 9 capsids. Injection of rAAV9-hADA intravenously or rAAV1-hADA intramuscularly into a mouse model of partial ADA deficiency demonstrated viral transduction of numerous tissues using rAAV9 and primarily skeletal muscle using rAAV1. Qualitatively, we observed ectopic hADA expression in skeletal muscle following rAAV1-hADA administration and in heart and kidney tissues following rAAV9-hADA injection. Time-course analyses of serum-based hADA activity revealed a trend toward increased ADA enzyme activity following vector administration. Lastly, the rAAV9-hADA vector propagated partial immune reconstitution, which increased in magnitude and diversity over time. Our data suggest that rAAV gene therapy strategies for the treatment of primary immunodeficiencies in general and, more specifically, for ADA-SCID may be feasible in the future.

Materials and Methods

Cloning of rAAV-hADA transgene

Critical to the success of this gene therapy endeavor was the cloning of a secretory tagged version of the *hADA* gene into a single-stranded rAAV vector. To that end, traditional cloning methods were used to generate several intermediate constructs and the cloning of the final plasmid, pTR2-CB-Igκ-hADA, and the final vector of interest, rAAV-hADA, from the initial retroviral plasmid, MND-MFG-hADA. The retroviral vector MND-MFG-hADA, provided by Dr. Donald Kohn at the University of Southern California–Keck School of Medicine (Los Angeles, CA), was the template for high-fidelity polymerase chain reaction (PCR). The hADA PCR product amplified from the MND vector was isolated on a 1.5% agarose gel and purified using a Qiagen (Valencia, CA) gel extraction kit, TA-cloned using the plasmid pCRTOPO2.1 (Invitrogen, Carlsbad, CA), and confirmed by DNA sequencing. Primers for all constructs were generated using Gene Runner software (Hastings Software, Hudson, NY). PCR primers used in generation of the hADA-TA construct were the forward sequence containing a 5′ *Hin*dIII restriction site, 5′GGAAGCTTAAGTCGAGGCATGGCCCAGACG3′, and the reverse sequence with a 3′ *Eco*RI restriction site, 5′CAGAATTCCGAGGTTCTGCCCTGCAGAGGC3′.

The hADA-TA construct was double-digested with *Hin*dIII and *Eco*RI restriction enzymes (New England Biolabs, Ipswich, MA) to excise the hADA transgene, which was then cloned into the pSecTag2 expression vector (Invitrogen) to generate the final transgene cassette and secretory version of the transgene. More specifically, the hADA transgene was cloned into the pSecTag2 vector backbone in-frame with an Igκ signal sequence upstream of the 5′ end of the transgene and a c-*myc*/poly-histidine tag downstream of the 3′ end of the trangene. The completed Igκ-hADA-c-*myc*/poly-His tag transgene cassette was cloned into a rAAV serotype 2 plasmid backbone to produce the plasmid, pTR2-CB-Igκ-hADA, shown in Fig. 1A. Flanking the transgene cassette were adeno-associated virus inverted terminal repeats upstream of the 5′ end of the cassette and downstream of the 3′ end.

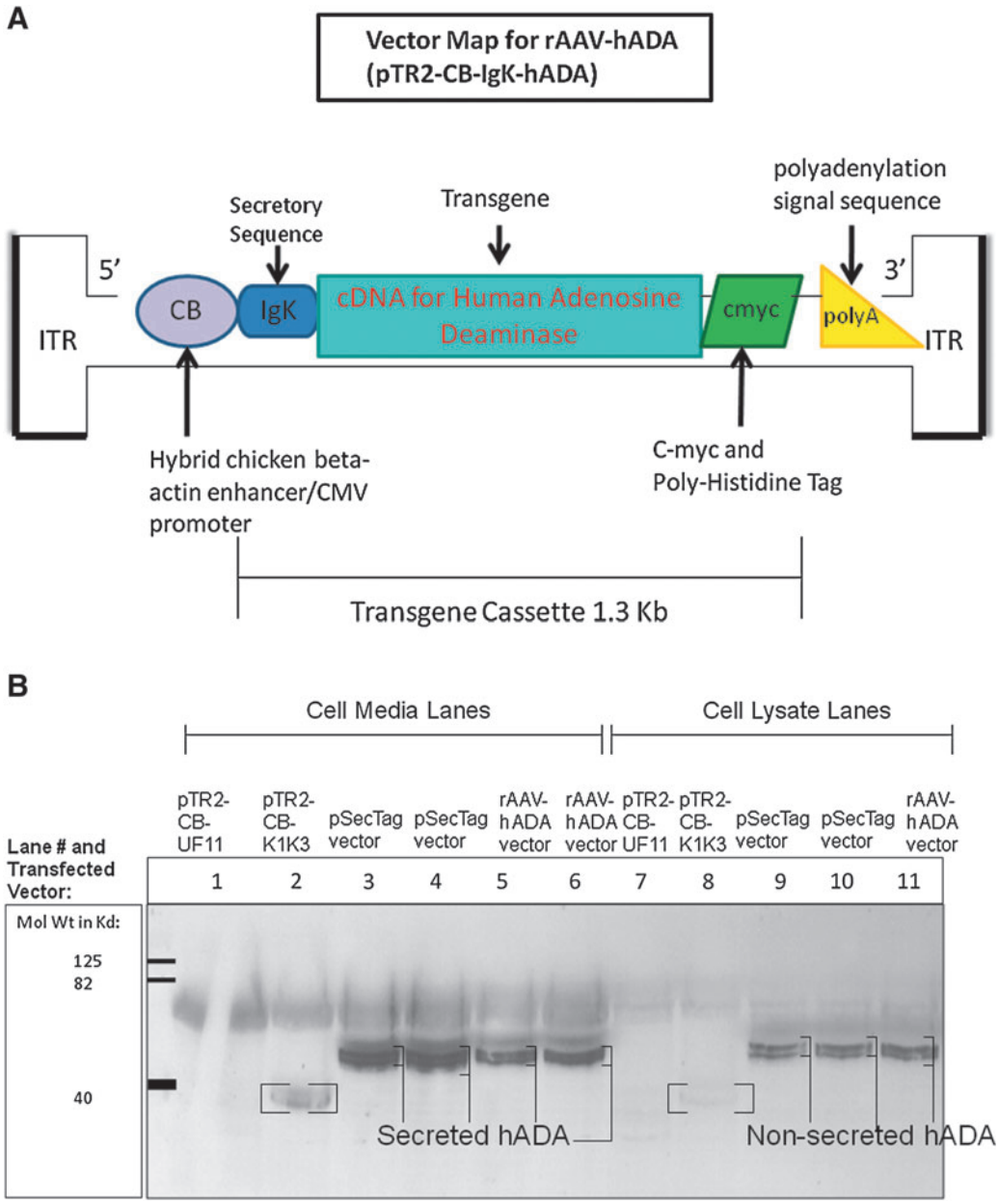

FIG. 1. (**A**) Map of the primary rAAV vector of interest, entitled rAAV-hADA, with all major components illustrated. This construct, otherwise known as pTR2-CB-Ig*κ*-hADA, was subsequently tested for the expression and secretion of hADA by subsequent transfection and western blot. CMV, cytomegalovirus; ITR, inverted terminal repeat. (**B**) Western blot confirming both the expression and secretion of hADA protein from pSecTag2-hADA and rAAV-hADA plasmids, as detected with an anti-*myc* tag antibody. All samples were obtained at 72 hr post-Lipofectamine 2000-mediated transfection of 293 cells. In cell media samples in lanes 3 and 4, bands representing secretory hADA from the pSecTag2-hADA construct were found at approximately 48 kDa. In cell media samples in lanes 5 and 6, bands representing secretory hADA from the rAAV-hADA vector were also observed at 48 kDa. Nonsecreted hADA expressed from the pSecTag2-hADA plasmid and found in 293 cell lysates are seen as multiple dark bands in lanes 9 and 10. Similarly, nonsecreted hADA protein, expressed from the rAAV plasmid and harvested from 293 cell lysates, was observed as multiple dark bands in lane 11. Negative control medium and cell lysate from 293 cells tranfected with pTR2-CB-UF11 (which expresses only intracellular GFP) was used in lanes 1 and 7, respectively, to demonstrate the absence of secreted and nonsecreted background c-*myc*-tagged protein at 48 kDa. Positive control bands for secreted and nonsecreted c-*myc*-tagged protein (designated by brackets) were observed strongly in lane 2 and less so in lane 8, respectively, representing c-*myc*-tagged angiostatin protein (derived from the construct pTR2-CB-K1K3 courtesy of the Flotte laboratory). The 316-amino acid angiostatin protein was found at the expected 36 kDa molecular mass.

Additional elements found upstream of the transgene cassette were a cytomegalovirus promoter and a chicken β-actin enhancer, whereas a polyadenylation signal sequence was downstream of the transgene cassette. The final rAAV-hADA plasmid was sequenced to confirm successful cloning of the secretory trangene cassette.

Transfections with hADA constructs

293T cells (a human embryonic kidney cell line expressing SV40 large T antigen) were transfected using a Lipofectamine 2000 (Invitrogen) strategy. Approximately $1–2\times10^5$ cells were plated into each well of six-well tissue culture dishes 24 hr before transfection and incubated at 37°C. For immunoblot analysis, medium was collected at time points between 24 to 72 hr after transfection, and cells were collected and lysed at 72 hr.

Western blotting

Samples of culture medium and 293 cell lysates were collected from 24 to 72 hr after transfection with two experimental vectors (pSecTag-hADA and pTR2-CB-Igκ-hADA), the positive control vector (pTR2-CB-UF11), and no vector. Samples were incubated with the primary antibody (monoclonal antibody [mAb]) and anti-c-*myc*-horseradish peroxidase (Invitrogen) and analyzed for fluorescence from bound anti-c-myc mAb conjugated to horseradish peroxidase (Invitrogen) using an enhanced chemiluminescence detection kit (Amersham Biosciences, Piscataway, NJ).

Production and purification of rAAV vectors

The rAAVplasmid, pTR2-CB-Igκ-hADA, was used for packaging in type 1 and type 9 capsids. All rAAV vectors were generated by the Vector Core in the Powell Gene Therapy Center at the University of Florida (Gainesville) as described previously. Physical titers (genome numbers) were determined by dot-blot, and infectious titers and extent of wild-type (WT) adeno-associated virus serotype 2 contamination were determined by infectious center assay.

Mouse model

There are no known naturally occurring animal models of ADA deficiency due to embryonic lethality, but two genetically altered ADA-deficient mouse models are available for study. Although the original ADA-deficient mouse model demonstrated profound immune deficiency and bone and renal defects, it can be rescued from embryonic lethality by transgenic placental hADA expression. However, these mice die of severe respiratory distress at 3 weeks of age. As a more viable model for study of immune reconstitution, mice partially ADA-deficient were generated that express hADA in the placenta and forestomach (ADA knockout [KO] mice). These mice display a poorly characterized partial immune deficiency with less severe pulmonary inflammation and an enhanced lifespan (Blackburn *et al.*, 1996, 1998; Chunn *et al.*, 2006).

Mouse colony

Frozen $ADA^{+/-}$ embryos of the strain *FVB;129-Ada<tm1Mw> Tg(PLFSADA)2465Rkmb/J* (JAX Mice and Services stock number 003297) were obtained from Jackson Laboratories (Bar Harbor, ME). All mice were bred in the University of Florida Cancer Genetics Research Center Breeding Suite. All mice were the offspring of $ADA^{+/-}$ breeding pairs.

Administration of rAAV vectors

The rAAV-hADA plasmid packaged in serotype 1 and 9 capsids was administered to ADA KO mice between 6 and 8 weeks of age by intramuscular or intravenous injection, respectively. Five ADA KO mice were anesthetized with 1.5–2.5% isoflurane inhalation and received via tail vein injection 3×10^{11} particles of rAAV9-hADA in 50–200 μl of sterile phosphate-buffered saline (PBS). An additional four ADA KO mice received 3×10^{11} particles of rAAV1-hADA in 25–100 μl of sterile PBS by intramuscular injection into the right quadriceps muscle. Three ADA KO mice were used as negative controls and received 200 μl of PBS by tail vein and intramuscular injections. Lastly, one ADA KO mouse was injected via the tail vein with 3×10^{11} particles of a positive control vector carrying the gene for green fluorescent protein (GFP) called rAAV9-GFP (UF11) (courtesy of the University of Florida Vector Core).

Collection of blood samples

Blood samples were obtained by facial vein or retro-orbital bleeds with the animal under 1.5–2.5% isoflurane anesthesia. For any given blood draw, no more than 10% of the total blood volume was collected. For an average mouse at 8–10 weeks of age and weighing 25 g, 50 μl of serum was obtained from 100 μl of blood. Blood was obtained on days 9, 30, and 45 following vector injection for analysis of serum ADA enzyme activity. EDTA-anticoagulated peripheral blood was obtained monthly and used for flow cytometry and complete blood count (CBC) measurements.

Genotyping via genomic DNA extraction and PCR

To facilitate genotyping, genomic DNA was isolated from tail tips for subsequent PCR analysis using the Qiagen DNeasy blood and tissue kit. Tail tips were subjected to overnight proteinase K treatment in the presence of Buffer AT and ethanol at 56°C. Vortex-mixed samples were added to DNeasy Mini spin columns and centrifuged at 8,000 rpm for 1 min. The columns were washed with Buffers AW1 and AW2 and spun at 8,000 rpm for 1 min and 14,000 rpm for 3 min, respectively. Buffer AE was then used to elute purified genomic DNA into microcentrifuge tubes for subsequent PCR procedures.

Following DNA extraction, three separate PCR procedures were used to genotype mice. PCR protocols were graciously provided by the Blackburn laboratory at the University of Texas in Houston. The first PCR procedure amplified 700 bp of the null *ADA* allele. Detection of the 700-bp band on a 2.5% agarose gel indicated the presence of either one or two mutant *ADA* alleles. Absence of this band indicated a WT $ADA^{+/+}$ animal. The forward primer sequence was 5′AGAGCA GCCGATTGTCTGTT, with a melting temperature of 64.0°C. The reverse primer sequence was 5′AGAATGGACCG GACCTTGAT, with a melting temperature of 64.5°C.

The second PCR procedure amplified 274 bp of the WT *ADA* allele. Detection of a 274-bp band on a 2.5% agarose gel

indicated either one or two WT *ADA* alleles. Absence of this band indicated homozygosity for two mutant *ADA* alleles. For this reaction, the forward primer sequence was 5′CCTCTGAGCCATGATTCTGA, with a melting temperature of 63.0°C, and the reverse primer sequence was 5′AGAATGGACCGGACCTTGAT, with a melting temperature of 64.5°C.

The third PCR procedure amplified 470 bp of the hADA transgene. Detection of a 470-bp band on a 2.5% agarose gel indicated the presence of the hADA transgene. For this reaction, the forward primer sequence was 5′AGCCAACG CAGACCCAGAGA, with a melting temperature of 69.5°C, and the reverse primer sequence was 5′GCAGGCCC TGGTTCACAAGA, with a melting temperature of 70.0°C.

Immunohistochemistry

At 90 and 120 days post-injection of the rAAV1-hADA or rAAV9-hADA vector, mice were euthanized, and liver, kidney, pancreas, spleen, heart, thymus, and bilateral quadriceps muscles were harvested. Tissues were either snap-frozen in liquid nitrogen for genomic DNA isolation or fixed in 10% neutral-buffered formalin for immunohistochemical analysis.

Tissues were fixed in neutral-buffered formalin for 12–24 hr, rinsed twice in 1×PBS for 5 min each, processed, embedded in paraffin wax, and sectioned at 4 μm thickness. Tissue sections were deparaffinized, rehydrated, blocked with 3% hydrogen peroxide in methanol for 10 min, and incubated with primary mAb at room temperature for 1 hr prior to analysis.

To detect vector-mediated hADA expression, samples were first incubated in Antigen Retrieval Citra Solution (Biogenex, San Ramon, CA) for 30 min, rinsed in Dako Wash Buffer (1×Tris-buffered saline with 0.05% Tween) (DakoCytomation, Glostrup, Denmark), blocked with Background Sniper (Biocare Medical, Concord, CA) for 15 min, and rinsed in wash buffer. Rabbit anti-hADA mAb (Atlas Antibodies, Stockholm, Sweden) and normal rabbit immunoglobulin (Vector Laboratories, Burlingame, CA), as a negative control, were diluted 1:800 in Antibody Diluent (Zymed, Invitrogen) and incubated with tissue samples followed by rinses in wash buffer. The secondary mAb, Mach 2 rabbit–horseradish peroxidase polymer (Biocare Medical), was added to tissue samples at room temperature for 30 min followed by rinses in wash buffer. Bound mAb was detected using the Cardassian 3,3′-diaminobenzidine tetrahydrochloride chromagen method (Biocare Medical). Tissues were counterstained with hematoxylin (Vector Laboratories), dehydrated, coverslipped, and scanned using the Aperio (Vista, CA) ScanScope CS Digital System.

No antigen retrieval was required to detect GFP in tissues injected with the UF11 vector. Tissues were blocked as with hADA detection, and rabbit anti-GFP mAb diluted 1:40,000 (Abcam, Inc., Cambridge, MA) was used for detection. Straight diluent was used as the negative control. The remaining assay steps were the same as for hADA detection.

Flow cytometry

Fresh mouse peripheral blood was collected monthly via facial vein bleeds. Fifty microliters of EDTA-anticoagulated blood, mixed with a cocktail of mAbs to CD19, CD3, CD4, CD8, and NK1.1 (eBioscience, San Diego, CA) conjugated to allophycocyanin, fluorescein isothiocyanate, PacificBlue, phycoerythrin, or phycoerythrin-Cy7, was lysed in red blood cell lysis buffer. The supernatants were analyzed on a BD Biosciences (San Jose, CA) SLR 11-color flow cytometer using FACS Diva software in the Flow Cytometry Core of the University of Florida Cancer Genetics Research Center.

Real-time quantitative PCR

Genomic DNA isolation from flash-frozen liver, stomach, spleen, kidney, pancreas, skeletal muscle, lung, and heart samples was done using the Qiagne DNeasy tissue kit. DNA concentrations were determined by ultraviolet spectrophotometry (BioPhotometer, Eppendorf, Hamburg, Germany). Vector sequences were detected using *Taqman* real-time PCR (Applied Biosystems, Carlsbad). One microgram of genomic DNA was used in quantitative PCR procedures. Vector-specific primer pairs and a *Taqman* probe were designed to bind to the cytomegalovirus enhancer/chicken β-actin promoter. Standard curves were established after spiking with the CBAT plasmid using triplicate samples. The technique sensitivity was 100 copies per microgram of input DNA. Reaction conditions were those recommended by Perkin-Elmer (Waltham, MA)/Applied Biosystems. Quantitative PCR was performed using the ABI *Taqman* 7900HT (Song *et al*., 2002; Poirier *et al*., 2004).

ADA enzyme activity assay

The ADA assay kit (catalog number DZ117A, Diazyme Laboratories, Poway, CA) was used to determine serum hADA enzyme activity from mice receiving injections of PBS, control vector, or experimental rAAV-hADA vectors. The ADA activity assay measures enzyme-mediated deamination of adenosine to inosine, which is converted to hypoxanthine by purine nucleoside phosphorylase. Xanthine oxidase then catalyzes formation of uric acid and hydrogen peroxide from hypoxanthine. The resulting hydrogen peroxide is mixed with 4-aminoantipyrine and *N*-ethyl-*N*-(2-hydroxy-3-sulfopropyl)-3-methylaniline in the presence of peroxidase, which generates quinone dye, the absorbance of which is monitored kinetically. The change in absorbance over time was used to determine ADA activity.

Results

Preliminary studies

Unpublished studies upon which experiments were predicated were limited by the availability of viable ADA KO animals. Initially, rAAV1-hADA at dosages of 1×10^{10} ($n=4$) and 1×10^{11} ($n=6$) vector particles was given by intramuscular injection to 10–12-week-old WT animals of the identical strain described for this experiment. The animals were followed for 60 days, and a modest degree of gene delivery to skeletal muscle (no higher than 1×10^{3} vector genomes [vg]/μg of total DNA) was observed. Limited protein expression was observed in skeletal muscle by immunohistochemistry, compared with PBS-injected control mice ($n=3$). Background serum ADA activity confounded assessment of vector-driven enzyme secretion. Four mice were administered a control vector, rAAV1-hAAT, containing the gene for human α-1 antitrypsin (courtesy of the Flotte

laboratory). Abundant gene delivery (5×10^3–4×10^5 vg) and protein expression were observed in control animals.

We then turned our attention to testing the serotype 9 vector and were able to generate our first ADA KO animals. rAAV9-hADA was administered by intravenous injection at 1×10^{11} vector particles to ADA KO mice ($n=2$) and ADA WT mice ($n=2$) at 6–8 weeks of age. A positive control vector, rAAV9-GFP (UF11), containing the gene for GFP, was administered by intravenous injection to one ADA KO and one WT mouse. Also, one PBS-injected ADA KO and one WT mouse served as negative controls. The experiment continued until 60 days post-injection. Abundant gene delivery in ADA KO mice compared with PBS controls was detected (2×10^3–4×10^4 vg/μg of total DNA) in many tissues (heart, kidney, liver, spleen, pancreas, and skeletal muscle). Gene delivery in the WT animals ranged from 1×10^3 to 1×10^5 vg/μg of DNA in identical tissue types. Abundant hADA expression in cardiac muscle in ADA KO and WT mice was also observed compared with that of PBS control mice ($n=2$). Serum ADA enzyme activity decreased on average from 5.2 to 2.3 units over 60 days in ADA KO negative controls, but average ADA activity increased modestly from 5 to 6.5 units for vector-injected ADA KO mice. Similarly, slight decreases in average lymphocyte counts for control animals and slight increases over time for treated animals were observed.

Overall, these early experiments provided the initial data supporting gene delivery and expression in our animal model and suggested further analysis was necessary at higher vector dosages and in more ADA KO animals to observe any trends in ADA enzyme activity or immune reconstitution.

hADA constructs mediate hADA expression and secretion in vitro

Following cloning of pSecTag2-hADA and rAAV-hADA plasmid constructs, the ability of each construct to express and secrete hADA protein in tissue culture was evaluated. Expression of hADA protein was a critical step in evaluating viability of the hADA constructs for any attempt at *in vivo* preclinical gene transfer, but equally as important was the need to confirm secretion of hADA by transfected 293 cells *in vitro*. Immunoblots of culture media and cell lysates 72 hr after transfection confirmed hADA protein expression and secretion *in vitro* (Fig. 1B). Secreted hADA at the anticipated molecular mass of 48 kDa from 293 cells transfected with pSecTag2-hADA and rAAV-hADA constructs was readily detected with an anti-*myc* tag antibody. Nonsecreted hADA in lysates of cells transfected with either pSecTag2-hADA plasmid or rAAV-hADA plasmid was also observed. Immunoblot data for the preliminary pSecTag2-hADA construct and the final rAAV-hADA constructs demonstrated abundant cellular expression and substantial secretion of hADA *in vitro*.

Characterization of the immune deficiency in ADA KO mice

Prior to *in vivo* testing of rAAV vectors packaged in serotype 1 and 9 capsids, characterization of the partial immune deficiency in a mouse model of ADA deficiency was done. This characterization was critical for three reasons: (1) If a significant immune deficiency was seen in ADA KO mice, then the likelihood that rAAV gene therapy strategy may lead to immunological benefit would be substantial; (2) if the immune deficiency was minimal compared with ADA WT or ADA heterozygous mice, then the likelihood of observing substantial immune reconstitution in ADA KO mice may prove unrealistic; and (3) if the immunodeficiency observed in ADA KO mice was severe, then single-stranded rAAV-based gene therapy, even if administered at earlier than 6–8 weeks of age, may not be able to progress in time to provide sufficient secreted hADA to rescue or clinically benefit ADA KO mice. With these considerations in mind, flow cytometry and CBC measurements were done to characterize the immune deficiency described by Jackson Laboratories for this ADA KO mouse model, although not published in the literature. Numbers of peripheral blood cells expressing CD19, CD3, CD4, CD8, and CD16 were measured in ADA KO, ADA heterozygous, and ADA WT mice over time as surrogate markers for immunocompetence. Analyses of flow cytometry data and CBC collected over a 5-month period from ADA KO mice ($n=4$) and ADA WT or ADA heterozygous littermates ($n=3$) between the ages of 4 to 8 months suggest that the absolute lymphocyte count (ALC) values and numbers of B cells and T-cell subsets in ADA KO mice were substantially lower than in ADA WT controls (Fig. 2). The average ALC values of ADA WT mice were two- to threefold greater than that of ADA KO animals ($p<0.0001$), and numbers of B cells and T-cell subsets in ADA WT mice were two- to fourfold higher than in ADA KO mice ($p<0.0001$ for CD19 cells, $p<0.0001$ for CD3 cells, $p=0.0003$ for CD4 cells, $p<0.0001$ for CD8 cells) with the exception of NK cells ($p=0.8875$).

Recombinant AAV-hADA vectors mediate substantial hADA expression in vivo *in cardiac and skeletal muscle as well as kidney*

rAAV1-hADA and rAAV9-hADA vectors were administered to ADA KO mice to facilitate gene delivery, protein expression, enhanced serum enzyme activity, and immune reconstitution. At day 120 post-injection, ADA KO mice were sacrificed, and necropsies were done to harvest tissues for quantitative PCR as indicators of gene delivery and transduction efficiency. The degree of gene delivery varied from tissue to tissue and mouse to mouse in all experimental groups (Table 1). Negative control tissue (with the exception of one sample of pancreas) from PBS-injected ADA KO mice did not show significant levels of background vector.

For mice injected with rAAV9-hADA in this experiment, gene delivery was most efficient in heart and lung with substantial vg numbers in all injected animals (Table 1). The vector copy numbers ranged from 1×10^3 to 7×10^3 in heart to 1.1×10^3 to 8.5×10^3 for lung. Substantial vg numbers were found in kidney (5.8×10^2–1×10^4 vg), liver (2×10^2–2×10^3 vg), pancreas (as high as 2×10^3 vg), and skeletal muscle (2×10^2–1.1×10^4 vg), although levels were not as consistent as those observed for heart and lung. Spleen, stomach, and thymus tissues showed no consistent indication of substantial gene delivery. In contrast, in ADA KO mice injected with rAAV1-hADA, vector genomes were found consistently only in the primary target tissue, quadriceps skeletal muscle (6×10^3–1.6×10^5 vg), although in some cases vector migrated through

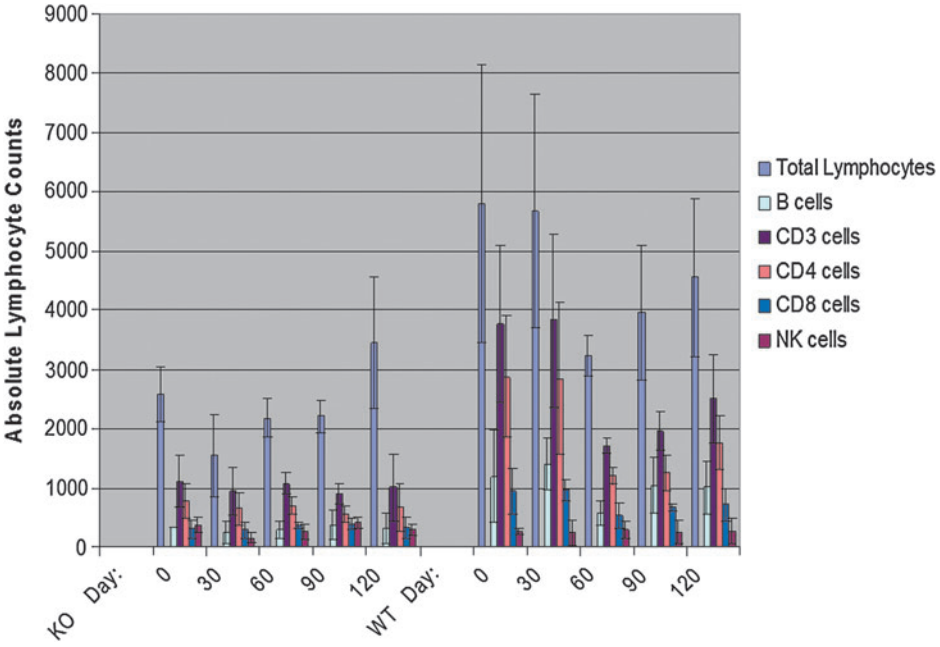

FIG. 2. Quantification of total lymphocytes and immunological cell subsets in ADA-SCID KO and WT mice over time. The relative lymphocyte populations of KO ADA-SCID mice (**left panel**) compared with their WT littermates (**right panel**) are shown over the course of 120 days. The mice were age-matched and followed from 4 months to 8 months old. The lymphocyte counts were obtained from CBC analyses and multiplied by lymphocyte subset percentages, derived from flow cytometry, to yield counts of each lymphocyte subset. Overall, even with substantial SDs, the data suggest that the total lymphocyte, B cell, $CD3^+$ cell, $CD4^+$ cell, and $CD8^+$ cell counts of the KO mice are substantially lower than those of the WT controls. Statistically, when all counts of immunological cells derived from the KO mice, over all time points, are compared with those of the WT mice, over all time points, significant differences with p values <0.05 were observed for total lymphocytes and all cell subsets with the exception of NK cells: total lymphocytes, $p < 0.0001$; B cells, $p < 0.0001$; CD3+ cells, $p < 0.0001$; CD4+ cells, $p = 0.0003$; CD8, $p < 0.0001$; NK cells $p = 0.8875$.

the circulation to other tissues such as liver and lung. Overall, moderate to abundant levels of rAAV9-mediated hADA delivery were achieved and persisted over a prolonged period of time in various tissues, especially heart, lung, liver, kidney, and skeletal muscle. Modest to high levels of rAAV1-mediated hADA delivery and long-term persistence were confined to skeletal muscle.

For ADA KO mice administered rAAV1-hADA, tropism of this serotype for skeletal muscle was observed as seen in numerous previous studies (Yan *et al*., 2005; Lu *et al*., 2006; Toromanoff *et al*., 2008). Intramuscular injection successfully delivered rAAV1 to the quadriceps muscle of ADA KO animals and resulted in substantial hADA protein expression in skeletal myofibers compared with control PBS-injected ADA KO animals on day 120 post-vector injection (Fig. 3). The banding pattern of numerous brown-staining muscle fibers with unstained fibers interspersed between stained fibers (Fig. 3A) is characteristic of rAAV vector-based protein expression (Yan *et al*., 2005; Lu *et al*., 2006; Toromanoff *et al*., 2008).

For ADA KO mice administered rAAV9-hADA, abundant hADA protein expression on day 120 post-vector injection was observed consistently in cardiac muscle compared with cardiac muscle from PBS-injected ADA KO animals (Fig. 4A–C). Variable levels of hADA staining of cardiomyocytes would likely correlate with substantial, but variable, hADA expression in individual cardiomyocytes. Given intravenous delivery of rAAV9-hADA, the innate ability of this serotype to cross endothelial barriers and target heart was anticipated and indicated by the results observed (Inagaki *et al*., 2006; Vandendriessche *et al*., 2007; Miyagi *et al*., 2008).

Substantial hADA expression was observed in kidney from rAAV9-hADA-injected ADA KO mice compared with kidney from PBS-injected ADA KO mice on day 120 post-vector injection (Fig. 4D–F). Abundant hADA staining throughout the renal medulla and pelvis was seen. Darkly stained cells likely represent epithelial cells in the collecting ducts and loops of Henle. Kidney, like cardiac muscle, is heavily vascularized and exposed to constant high blood flow. Consequently, exposure of kidney to rAAV9 may explain intense hADA expression in this tissue (Lipkowitz *et al*., 1999; Chen *et al*., 2003; Choi *et al*., 2010).

In ADA KO mice administered the positive control vector, rAAV9-GFP (UF11), identical tissues stained for GFP (Fig. 4). Hematoxylin and eosin staining was also done to assess qualitatively the presence or absence of immune responses at time of sacrifice, which could have been targeted to either the transgene or vector capsid. In no instance was a lymphocytic infiltrate observed.

Overall, this experiment provided demonstration of substantial hADA staining in skeletal muscle following administration of rAAV1-hADA and abundant consistent staining of cardiac muscle following rAAV9-hADA injection. These data suggest the skeletal and cardiac muscles are the primary sites of ectopic hADA expression and potentially secretion. Also, detection of hADA protein in kidney of rAAV9-injected mice suggests kidney may be a possible secondary site of hADA expression and secretion.

Enhanced serum hADA enzyme activity in rAAV-hADA-treated ADA KO mice

Serum ADA activity over the first 45 days in rAAV1-hADA- and rAAV9-hADA-treated ADA KO mice was more than that seen in control ADA KO mice, except for the day 9 rAAV1 group. Trends toward an increased ADA enzyme

Table 1. Gene Delivery Data, Describing Vector Copy Numbers in Various Murine Tissues, Collected at Sacrifice, on Day 120 Post-Injection of 3×10^{11} Particles of rAAV1-hADA, rAAV9-hADA, rAAV9-UF11 (GFP), or PBS, in ADA-SCID KO Mice

		Vector copy number in tissue (per μg of DNA)							*Vector copy number in tissue (per μg of DNA)*			
Mouse ID #	*Vector or PBS given*	*Pancreas*	*Skeletal muscle*	*Spleen*	*Stomach*	*Thymus*	*rAAV serotype*	*Day of sacrifice*	*Heart*	*Kidney*	*Liver*	*Lung*
36	PBS	4	28	0	1	0		120	3	0	0	0
27	PBS	26	34	0	9	0		120	0	1	0	0
41	PBS	583	66	2	1	5		120	6	0	0	26
Average			42.66667	0.666667	3.666667	1.666667			3	0.333333	0	8.666667
SD			20.42874	1.154701	4.618802	2.886751			3	0.57735	0	15.01111
29	Vector	2,340	5,922	667	92	12,073	9	120	7,178	1,303	1,921	8,484
30	Vector	2,643	11,268	2,244	116	15	9	120	3,864	588	251	1,273
40	Vector	64	703	100	23	88	9	120	1,631	752	944	1,253
28	Vector	533	724	188	46	213	9	120	3,011	1,328	1,545	1,112
31	Vector	NA	2,227	NA	NA	NA	9	120	NA	10,672	312	NA
Average		1,395	4,168.8	799.75	69.25	3,097.25			3,921	2,928.6	994.6	3,030.5
SD		1,286.485	4,503.37		42.35859	5,984.392			2,358.212	4,341.104		3,636.373
34	Vector	44	117,056	122	1	0	1	120	118	92	1,638	297
39	Vector	3,581	31,523	150	33	147	1	120	292	98	592	2,801
38	Vector	16	6,198	15	8	152	1	120	17	33	369	37
33	Vector	37	159,927	34	NA	24	1	120	NA	42	292	NA
Average		919.5	78,676	80.25	14	80.75				66.25	722.75	1,045
SD		1,774.373	71,998.18	65.84008	16.8226	80.01406				33.49005		1,526.287
35	Vector (+control, rAAV1-GFP)	4,116	43,981	1,460	647	8,804	1	120	2,042	1,716	13,551	36,000

Overall, with one exception being background rAAV in one sample of pancreas, consistent negative control values are found through low to absent background vector copy numbers in negative control tissues from PBS-injected mice. By contrast, substantial vector copy numbers were found in heart, lung, kidney, liver, pancreas, and skeletal muscle for KO mice administered type 9 control and experimental vectors, whereas abundant vector copy numbers were found in the skeletal muscle of KO mice given type 1 vector. These data indicate substantial gene delivery and transduction efficiency in multiple tissues for KO mice treated with rAAV9-hADA, and in skeletal muscle for KO mice given rAAV1-hADA, compared with KO mice administered PBS.

NA, not available.

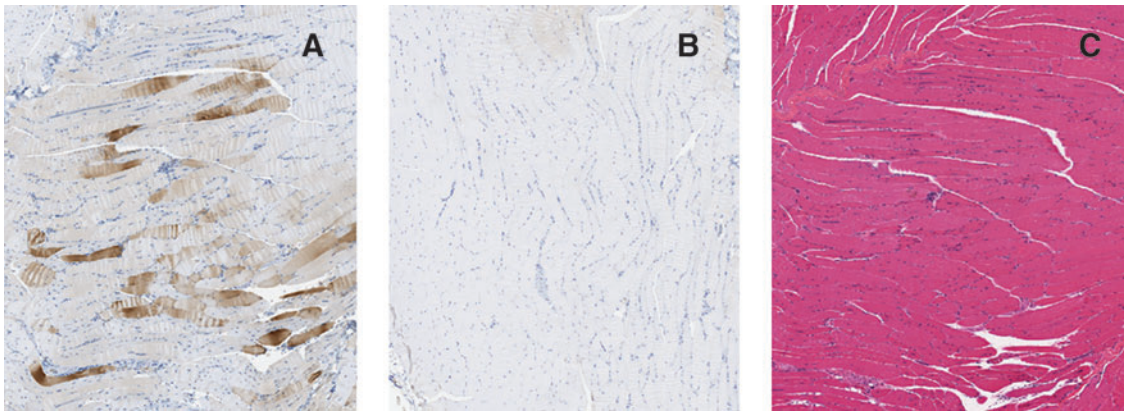

FIG. 3. Immunohistochemical staining for hADA and staining by hematoxylin and eosin in murine skeletal muscle, on day 120, following intramuscular injection of rAAV1-hADA or saline. (**A** and **B**) Representative images of immunohistochemical staining for hADA in skeletal muscle tissue of (**A**) vector-treated mouse ID #38 and (**B**) PBS-injected mouse ID #36. (**C**) Representative image of hematoxylin and eosin staining of skeletal muscle from mouse ID #38 on day 120 following intramuscular injection of rAAV1-hADA. Overall, substantial hADA expression was detected in the target skeletal muscle tissue of vector-treated versus untreated mice. Hematoxylin and eosin staining revealed no visible inflammatory infiltrates in response to vector or transgene.

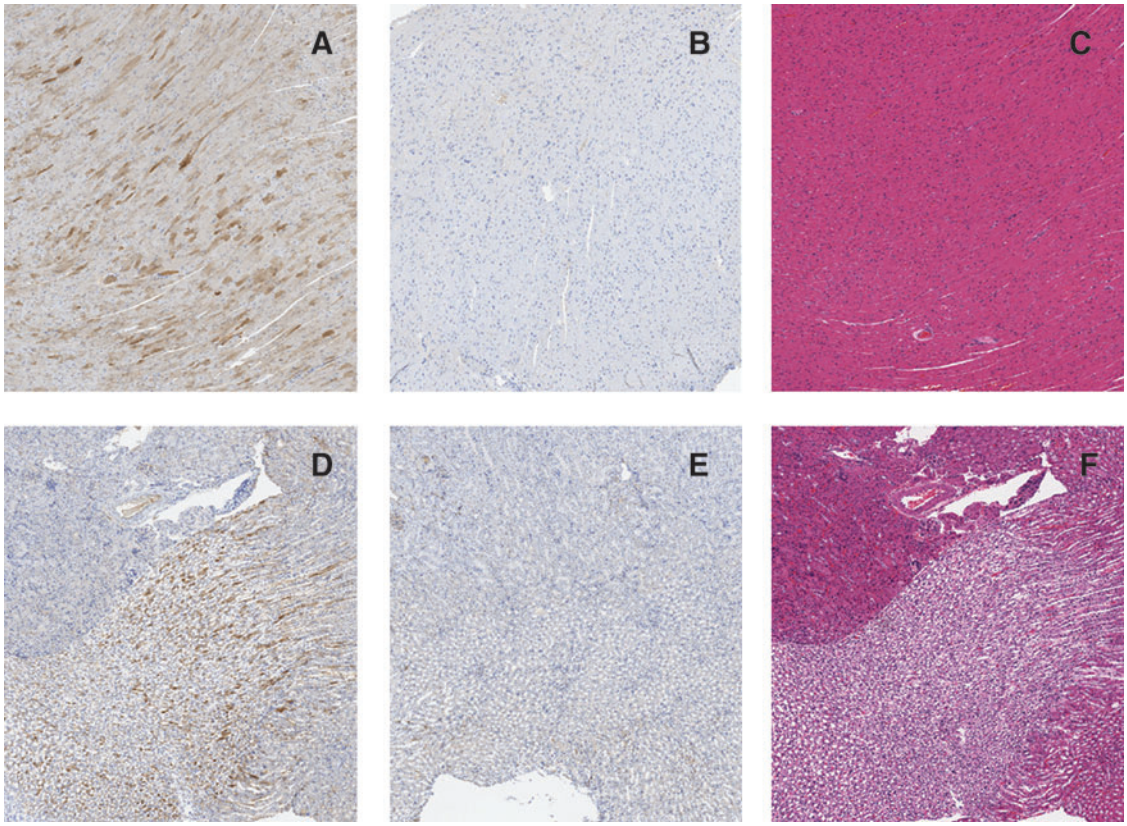

FIG. 4. Immunohistochemical staining for hADA and staining by hematoxylin and eosin of murine heart and murine kidney, on day 120, following intravenous injection of rAAV9-hADA or saline. (**A** and **B**) Representative images of immunohistochemical staining for hADA in cardiac muscle tissue of (**A**) vector-treated mouse ID #30 and (**B**) PBS-injected KO mouse ID #27. (**C**) Hematoxylin and eosin staining of the cardiac muscle tissue of vector-treated mouse ID #30. Overall, a substantial degree of hADA staining was observed throughout cardiac muscle tissue in treated versus untreated KO mice. No inflammatory infiltrates were observed upon hematoxylin and eosin staining of cardiac muscle, which would indicate a host immune response to vector or transgene. (**D** and **E**) Representative images of immunohistochemical staining for hADA in the kidney (renal medulla and pelvis) of (**D**) vector-treated mouse ID #40 and (**E**) PBS-treated mouse ID #27. (**F**) Representative image of hematoxylin and eosin staining in the kidney (renal medulla) of vector-treated mouse ID #40. Overall, staining for hADA revealed substantial protein expression in the renal medulla of at least one vector-treated KO mouse compared with untreated KO mice. No inflammatory infiltrate was observed upon hematoxylin and eosin staining, indicating no inflammatory response to vector or transgene was present.

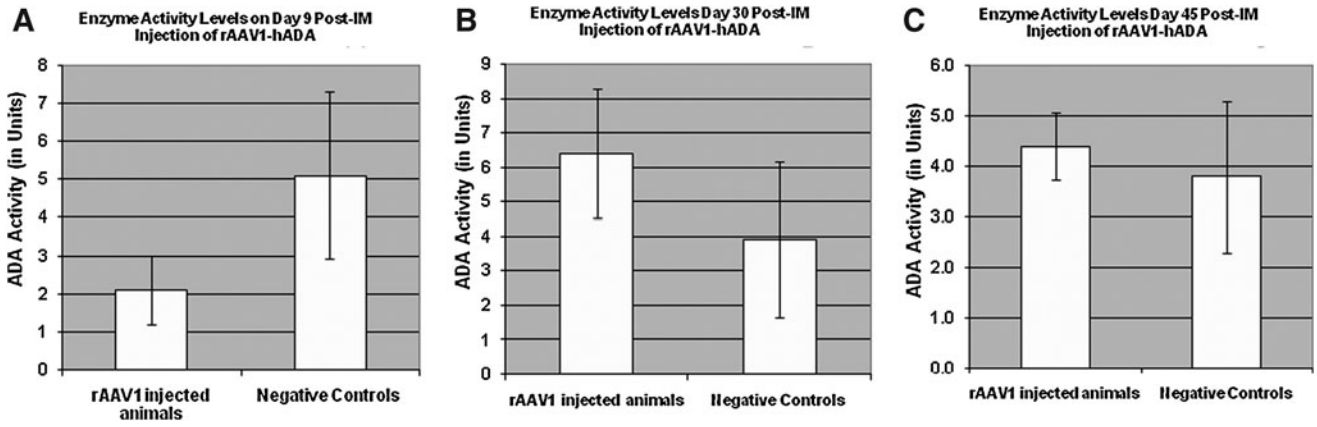

FIG. 5. Enzyme activity in harvested mouse serum on days 9, 30, and 45 following administration of rAAV1-hADA or lactated Ringer's PBS to ADA-SCID KO mice. (**A**) Serum hADA activity on day 9 post-vector injection is low relative to that of negative control mice, indicating either a lack of vector-driven enzyme activity or a relatively high degree of background enzyme activity. (**B**) Observed serum enzyme activity on day 30. At this time point, the average level of serum enzyme activity increases approximately threefold for vector-treated mice, whereas background ADA activity from PBS-injected mice remains relatively stable. (**C**) hADA activity found in mouse serum on day 45. At this final time point, enzyme activity in serum of treated animals decreases, whereas enzyme activity for the untreated animals remains stable at approximately 4 units. Overall, this time-course study suggests a trend of increasing and decreasing levels of serum ADA activity in treated versus untreated KO mice, which may parallel cycles of enzyme synthesis and degradation in the treated mice. However, given the large SDs, the observed trend is not statistically significant. Post-IM, post-intramuscular.

activity were greater in the rAAV9 group but did not reach statistical significance (Figs. 5 and 6). Background serum ADA activity in saline-injected ADA KO mice remained relatively constant over time, fluctuating no more than 1.3 units over the 45-day time course. In contrast, serum ADA activity for rAAV1-hADA-injected mice increased as much as 4.3 units from day 9 to day 30, which represented an average increase of 2.5 units. For rAAV9-hADA-injected mice, serum ADA activity remained above background as much as 4 units at each time point. ADA enzyme activity was variable, perhaps reflecting cycles of enzyme degradation and synthesis over time. These data, especially with parallel assessments of lymphocyte numbers following vector administration, suggested vector-derived serum-based hADA enzyme activity.

Substantial lymphocyte reconstitution in treated ADA KO mice

Just as with earlier lymphocyte enumeration in ADA KO versus ADA WT littermates, the immunological endpoints of interest following rAAV-hADA injection included determi-

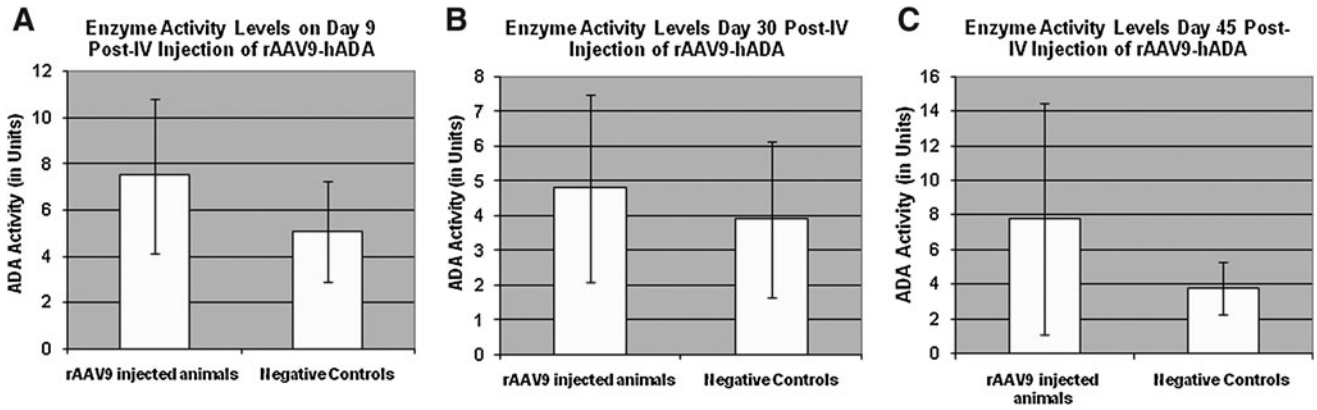

FIG. 6. Serum enzyme activity on day 9, 30, and 45 following rAAV9-hADA or lactated Ringer's PBS administration to ADA-SCID KO mice. (**A**) hADA activity in mouse serum on day 9. At this time point, the average level of enzyme activity is 2–3 units higher in treated versus untreated KO mice. (**B**) hADA activity on day 30. At this time point, the average level of ADA activity decreases in the treated mice, although enzyme activity remains relatively stable in the untreated mice. (**C**) Observed serum enzyme activity on day 45. On day 45, although the average level of ADA activity continues to remain stable at approximately 4 units for untreated mice, average enzyme activity increases to nearly 8 units in treated mice. Overall, this time-course study suggests a trend of increasing and decreasing levels of serum ADA activity in treated versus untreated KO mice, which may parallel cycles of enzyme synthesis and degradation in the treated mice. However, given the large SDs, the observed trend is not statistically significant. Post-IV, post-intravenous.

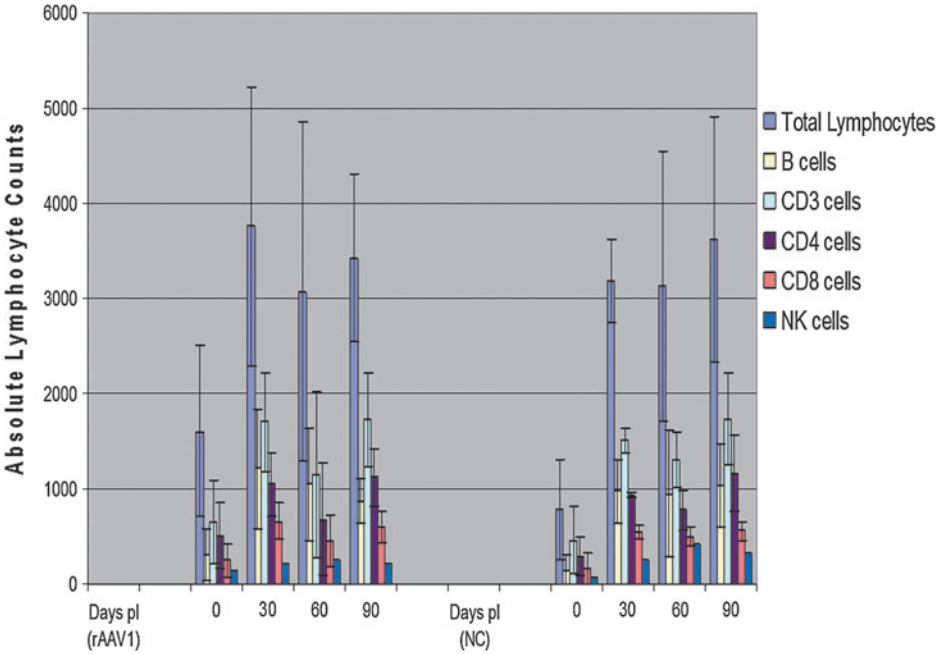

FIG. 7. Lymphocyte populations followed over a 90-day time course following intramuscular injections of rAAV1-hADA or lactated Ringer's PBS in ADA-SCID KO mice. (**Left panel**) Total lymphocyte and lymphocyte subset populations at monthly time points post-injection (pI) of rAAV1-hADA into KO mice. (**Right panel**) Equivalent lymphocyte populations for untreated KO mice administered PBS (negative control [NC]). Overall, a comparison of lymphocyte populations in the treated versus the untreated KO mice reveals no positive trend toward lymphocyte proliferation in the treated group.

nation of ALC values and B, CD3, CD4, CD8, and NK cell counts in mice at times points between 0 and 120 days post-injection. ADA KO mice injected with rAAV1-hADA did not have significantly increased ALC values or lymphocyte subsets compared with untreated mice (Fig. 7). In contrast, rAAV9-hADA-treated ADA KO mice showed progressive lymphocyte reconstitution over time (Fig. 8). ALC values and B, CD3, CD4, and CD8 cell populations in ADA KO mice injected with rAAV9-hADA demonstrated progressive increases in lymphocyte numbers and T-cell subsets over time compared with untreated ADA KO mice. Furthermore, ALC values and numbers of B cells and T-cell subsets in rAAV9-hADA-injected mice on day 90 were significantly greater than baseline values on day 0 (ALC, $p = 0.0038$; B cells, $p = 0.0120$; CD3 cells, $p = 0.0027$; CD4 cells, $p = 0.0025$; CD8 cells, $p = 0.0064$; NK cells, $p = 0.0004$). However,

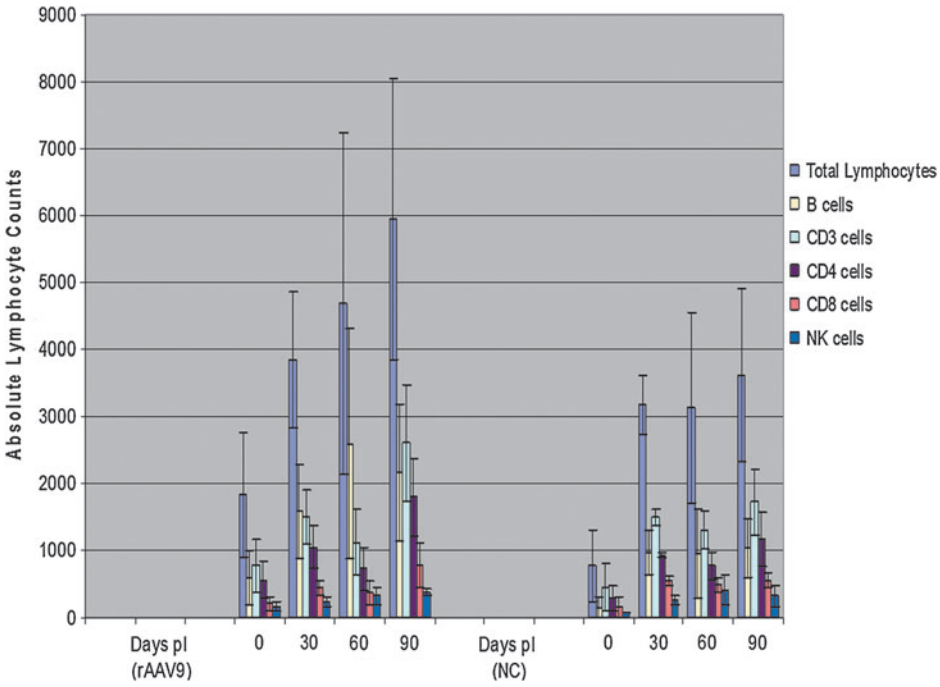

FIG. 8. Lymphocyte proliferation following intravenous injections of rAAV9-hADA vector or lactated Ringer's PBS in ADA-SCID KO mice. (**Left panel**) Total lymphocyte and lymphocyte subset counts, followed over 90 days, at 30-day intervals, in vector-treated KO mice (labeled "rAAV9"). (**Right panel**) Equivalent lymphocyte populations, at equivalent time points, in PBS-injected, negative control (NC), knockout mice. It is interesting that a positive, progressive trend in total lymphocytes as well as lymphocyte subset populations was observed in the treated versus the untreated KO mice. Total lymphocyte, B cell, $CD3^+$ cell, $CD4^+$ cell, and $CD8^+$ cell counts followed over time, and following injection of vector or PBS, show a positive, progressive, increasing trend for the treated animals relative to the untreated animals. Although the average B-cell counts decrease by day 90 for treated animals, counts are still substantially higher than the B-cell counts of untreated mice. NK-cell counts, followed over time, and following injection of vector or PBS, show a steady, but weaker, positive trend over the 90-day experiment for the treated relative to the untreated animals. pI, post-injection.

statistical significance proved challenging when assessing lymphocyte counts between rAAV9-hADA-treated versus untreated ADA KO animals.

Discussion

In summary, our data following rAAV1-hADA injection did not indicate immune reconstitution, at least as assessed by lymphocyte numbers, in vector-injected ADA KO mice compared with control ADA KO mice. However, average total lymphocyte and lymphocyte subset counts increased over time in ADA KO mice following rAAV9-hADA administration, indicating substantial, progressive, and prolonged reconstitution of lymphocytes in vector-treated ADA KO mice compared with control ADA KO mice.

These observed trends indicated that perhaps transduced tissue of the heart, or the combination of multiple transduced tissue types such as heart, liver, and kidney, serves as a superior site or sites, respectively, of ectopic hADA expression/secretion following rAAV9-hADA administration, compared with skeletal muscle–driven ectopic hADA expression/excretion following rAAV1-hADA injection. It is interesting that, if confirmed by ongoing experiments, B cells appeared to be the first lymphocyte subset to proliferate following rAAV9-hADA injection in treated KO mice compared with untreated KO mice (see the Day 60 data in Fig. 8). Coincidentally, B cells are also the lymphocyte type in ADA-SCID that typically develops first in patients with ADA-SCID treated with PEG-ADA. Thus, any serum-based detoxification would be predicted to facilitate B-cell proliferation ahead of T-cell proliferation, which requires more time because of T-cell ontogeny. Consistent with this prediction was the reconstitution of additional lymphocyte subsets, including $CD3^+$ and $CD4^+$ cells, only after B-cell proliferation (see the Day 90 data in Fig. 8).

However, further studies must be pursued to confirm or deny the significance of the observed immunological trends and assess any benefit to immune function that may or may not accompany the observed trends. Further analysis of serum ADA activity, including metabolic analyses such as adenosine, deoxyadenosine, and deoxy-ATP levels, and the potential development of an ADA-enzyme-linked immunosorbent assay for quantification of serum ADA protein may further corroborate the observed trends.

It is interesting that the widespread distribution of rAAV9-hADA vector and observed expression of hADA in tissues such as heart and kidney may one day provide therapeutic benefits unseen previously for retroviral gene therapies. First, rAAV-mediated gene delivery and hADA protein expression in various murine target tissues offer the potential for enzyme secretion into the circulation and potential benefit of direct systemic detoxification. Second, the expression of hADA in numerous target tissues may offer sites that can serve as metabolic depots or metabolic "sinks," as Carbonaro *et al*. (2006) recently described in a lentiviral study directed at amelioration of ADA-SCID through overexpression of ADA in liver and lung in a more severely immune-deficient mouse model of this disease. In other words, similar to the lentiviral study of Carbonaro *et al*. (2006), regional sites of rAAV-mediated intracellular overexpression of hADA could provide not only local benefit to a variety of tissues, but also handle detoxification of circulating body metabolites. This may ultimately produce more systemic benefit, including restoration of lymphocyte populations and function. The potential for single-stranded, self-complementary, or mutant rAAV vectors to provide both local and systemic benefits offers more global approaches to amelioration of this potentially fatal disease, which adversely affects not only the immune system but also numerous nonimmunological tissues (Carbonaro *et al.*, 2006).

One of the difficulties observed in this study was the background ADA activity observed in the serum of ADA KO control mice. The most likely explanation for background enzyme activity in negative control ADA KO mice may be related to natural cycles of cellular growth, proliferation, death, and degeneration inherent to all tissues, especially those that are rescued in this ADA KO mouse model, including the forestomach and intestine. Over time, degradation of foregut-derived tissues, stomach, duodenum, and intestine may release proteins such as ADA into the extracellular space and ultimately the blood. Subsequently, when blood is harvested for serum analysis, relatively stable levels of background ADA protein and enzyme activity may be present. This possible explanation is supported by the observation that background ADA activity in negative control mouse sera remained relatively steady from time point to time point (Blackburn *et al.*, 1996).

The large SDs in ADA activity observed for the experimental groups relate directly to number of animals used as well as the variability of serum ADA activity in different ADA KO animals at any given time point.

Also, once the serotype 9 vector was administered, migration of the vector through the bloodstream to the different organs and tissues may have varied and led to substantial SDs and lack of statistical significance observed for collected enzyme activity data. In some experimental mice, the vector may have migrated more efficiently to some tissues than to others. The observed quantitative PCR data illustrate this variability through variation in vector copy number observed for heart, liver, pancreas, skeletal muscle, and kidney tissues between mice in the same experimental group. In several mice of the rAAV9-hADA experimental group, vector transduction may have been superior in heart and kidney tissues and less substantial in liver and skeletal muscle; in other mice of the same experimental group, the pattern of vector transduction may have been the opposite. In this case, protein expression may very well have occurred in various tissues. However, the ability of different cell types to secrete protein and influence serum ADA activity may vary substantially. For example, in mice treated with the rAAV9 vector, in which substantial vector copy numbers could be found in tissues with high capacity for secretion, substantial protein expression coupled with secretion may have occurred. However, for mice also treated with rAAV9 vector in which substantial vector copy numbers could be found in tissues with lower capacity for secretion, protein may have been expressed but not secreted. Therefore, in the former group of rAAV9-treated mice, serum ADA activity may have been substantially higher than in the latter group of rAAV9-treated mice. A large SD for the calculated average levels of ADA activity in treated mice may have resulted making a statistically significant difference with average ADA activity in untreated $ADA^{-/-}$ mice difficult to observe.

Another challenge faced in these experiments was with observed phenotypic heterogeneity among $ADA^{-/-}$ mice. Overall, the partial immune deficiency of this $ADA^{-/-}$ model on an individual mouse basis appears to vary substantially from mouse to mouse and over time. This conclusion is based upon the initial immunological profile comparing $ADA^{-/-}$ mice to $ADA^{+/+}$ or $ADA^{+/-}$ mice, the baseline pre-injection assessment of the immunological status of $ADA^{-/-}$ mice to undergo vector treatment, and the monitoring of lymphocyte counts from PBS-injected mice. Immunological analysis of a given untreated $ADA^{-/-}$ mouse (confirmed through genotyping) over time or by comparison with additional untreated KO mice at one given point in time demonstrated that total lymphocyte and subset counts can vary broadly from hundreds of cells to over thousands of cells. One may conclude that the nature of the partial immune deficiency in this mouse model can vary substantially between individual mice and over time. This observed phenotypic heterogeneity helped contribute to average lymphocyte counts (among groups of untreated as well as vector-treated $ADA^{-/-}$) with large SDs, which in turn confounded analyses of statistical significance.

Yet, despite challenges with the murine phenotype and enzyme activity, the safety of these rAAV vectors was observed for all *in vivo* experiments. Two $ADA^{-/-}$ mice died during this experiment at the end of the experimental period, but both had experienced recent, heavy blood loss during facial and retro-orbital bleeds that were conducted under anesthesia. The bleeds were meant to facilitate enzyme activity, flow cytometry, and CBC analyses. However, the degree of fluid loss from the bleeds in two mice for which blood clotting may have proved difficult likely resulted in the two mouse deaths. Of the remaining mice used to date for testing of the rAAV vectors, all remained alive and well until their respective dates of sacrifice. This low toxicity for rAAV vectors is consistent with numerous preclinical and clinical rAAV studies.

Overall, rAAV-based gene therapy for ADA-SCID shows promise in preclinical studies conducted using a partially immune-deficient mouse model. A transgene cassette, composed chiefly of a c-*myc*/polyHis-tagged secretory version of the hADA gene, was cloned into single-stranded rAAV serotype 2 cloning vector to generate the plasmid, pTR2-CB-Igκ-hADA. This plasmid was tested in tissue culture and shown to express and secrete hADA protein. Then, a partially immune-deficient mouse model of ADA-SCID was successfully characterized by PCR-based genotyping and flow cytometry/CBC analysis–based phenotyping. The rAAV-hADA plasmid (pTR2-CB-Igκ-hADA) was then packaged into serotype 1 and 9 capsids and administered *in vivo* by intramuscular or intravenous injection, respectively, to $ADA^{-/-}$ mice. Several endpoints were analyzed over time periods that extended up to 120 days. These endpoints included confirmation of long-term, moderate gene delivery and transduction efficiency, as well as qualitative observations of vector-mediated hADA expression in skeletal muscle, cardiac muscle, kidney, and liver tissues. Subsequent serum-based analysis of enzyme activity revealed a trend towards increased levels of ADA activity in experimental vector-injected $ADA^{-/-}$ animals compared with control $ADA^{-/-}$ mice over time. This observed trend was not statistically significant but was corroborated by the final endpoint for this study, an analysis of lymphocyte reconstitution following rAAV injection. Although the data from this experiment revealed no trend or immune reconstitution for $ADA^{-/-}$ mice that received the rAAV1-hADA vector, a partial, progressive, prolonged, reconstitution of lymphocytes was indicated for $ADA^{-/-}$ mice that received the rAAV9-hADA vector. Further studies are needed, but the data presented here support the feasibility of an rAAV-based gene therapy for ADA-SCID and for primary immune deficiencies as a whole.

Acknowledgments

We thank Dr. Donald Kohn for his kind gift of MND-MFG-hADA plasmid. We also thank Dr. Michael Blackburn for his PCR-based genotyping assay for the ADA-SCID mouse model and Dr. Martha Campbell Thompson with the Molecular Pathology Core at the University of Florida for the beautiful imaging and immunohistochemistry. The animal colony breeding and maintenance could not have been done without the assistance of Ryan Fiske, Travis Cossette, and the entire staff of the University of Florida Animal Care Services. Flow cytometry was performed under the guidance and with the devoted assistance of Steve McClellan at the University of Florida Flow Cytometry Core. Also critical to this research was the University of Florida Toxicology Core for their efforts and quantitative PCR data. Lastly, we are grateful for the work of Dr. Barry Byrne, Mark Potter, and the entire University of Florida Vector Core for their packaging and titrating of our rAAV vectors.

Author Disclosure Statement

No competing financial interests exist.

References

Aitken, M.L., Moss, R.B., Waltz, D.A., *et al*. (2001). A phase I study of aerosolized administration of tgAAVCF to cystic fibrosis subjects with mild lung disease. Hum. Gene Ther. 12, 1907–1916.

Aiuti, A. (2004). Gene therapy for adenosine-deaminase-deficient severe combined immunodeficiency. Best Pract. Res. Clin. Haematol. 17, 505–516.

Aiuti, A., Cassani, B., Andolfi, G., *et al*. (2007). Multilineage hematopoetic reconstitution without clonal selection in ADA-SCID patients treated with stem cell gene therapy. J. Clin. Invest. 8, 2233–2240.

Baum, C. (2007). Insertional mutagenesis in gene therapy and stem cell biology. Curr. Opin. Hematol. 14, 337–342.

Baum, C., von Kalle, C., Stalle, F.J., *et al*. (2004). Chance or necessity? Insertional mutagenesis in gene therapy and its consequences. Mol. Ther. 9, 5–13.

Blackburn, M.R., Datta, S.K., and Kellems, R.E. (1998). Adenosine deaminase-deficient mice generated using a two-stage genetic engineering strategy exhibit a combined immunodeficiency. J. Biol. Chem. 273, 5093–5100.

Blackburn, M.R., Datta, S.K., Wakamiya, M, *et al*. (1996). Metabolic and immunologic consequences of limited adenosine deaminase expression in mice. J. Biol. Chem. 271, 15203–15210.

Booth, C.H., Hershfield, M., Notarangelo, L., *et al*. (2007). Management options for adenosine deaminase deficiency; proceeding of the EBMT satellite workshop (Hamburg, March 2006). Clin. Immunol. 123, 139–147.

Bushman, F.D. (2007). Retroviral integration and human gene therapy. J. Clin. Invest. 117, 2083–2086.

Carbonaro, D.A, Jin, X., Petersen, D., *et al*. (2006). In vivo transduction by intravenous injection of a lentiviral vector expressing human ADA into neonatal ADA gene knockout mice: A novel form of enzyme replacement therapy for ADA deficiency. Mol. Ther 13, 1110–1120.

Cavazzana-Calvo, M., and Fischer, A. (2007). Gene therapy for severe combined immunodeficiency: Are we there yet? J. Clin. Invest. 117, 1456–1465.

Chen, S., Agarwal, A., Glushakova, O.Y., *et al*. (2003). Gene delivery in renal tubular epithelial cells using recombinant adeno-associated viral vectors. J. Am. Soc. Nephrol. 14, 947–958.

Choi, J.O., Lee, M.H., Park, H.Y., and Jung, S.C. (2010). Characterization of Fabry mice treated with recombinant adeno-associated virus 2/8-mediated gene transfer. J. Biomed. Sci. 17, 26.

Chunn, J.L., Mohsenin, A., Young, H.W., *et al*. (2006). Partially adenosine deaminase-deficient mice develop pulmonary fibrosis in association with adenosine elevations. Am. J. Physiol. Lung Cell. Mol. Physiol. 290, L579–L587.

Cideciyan, A.V., Hauswirth, W.W., Aleman, T.S., *et al*. (2009). Vision 1 year after gene therapy for Leber's congenital amaurosis. N. Engl. J. Med. 361, 725–727.

Conlon, T.J., and Flotte, T.R. (2004). Recombinant adeno-associated virus vectors for gene therapy. Expert Opin. Biol. Ther. 4, 1093–10101.

Dave, U.P., Jenkins, N.A., and Copeland, N.G. (2004). Gene therapy insertional mutagenesis insights. Science 303, 333.

Duan, D., Sharma, P., Yang, J., *et al*. (1998). Circular intermediates of recombinant adeno-associated virus have defined structural characteristics responsible for long-term episomal persistence in muscle tissue. J. Virol. 72, 8568–8577.

Flotte, T.R. (2005). Adeno-associated virus-based gene therapy for inherited disorders. Pediatr. Res. 58, 1143–1147.

Flotte, T.R. (2007). Gene therapy: The first two decades and the current state-of-the-art. J. Cell Physiol. 213, 301–305.

Flotte, T.R., Afione, S.A., Conrad, C., *et al*. (1993). Stable in vivo expression of the cystic fibrosis transmembrane conductance regulator with an adeno-associated virus vector. Proc. Natl. Acad. Sci. U.S.A. 90, 10613–10627.

Flotte, T.R., Afione, S.A., and Zeitlin, P.L. (1994). Adeno-associated virus vector gene expression occurs in nondividing cells in the absence of vector DNA integration. Am. J. Respir. Cell. Mol. Biol. 11, 517–521.

Flotte, T.R., Brantly, M.L., Spencer, L.T., *et al*. (2004). Phase I trial of intramuscular injection of a recombinant adeno-associated virus alpha 1-antitrypsin (rAAV2-CB-hAAT) gene vector to AAT-deficient adults. Hum. Gene Ther. 15, 93–128.

Flotte, T., Carter, B., and Conrad, C., *et al*. (1996). A phase I study of an adeno-associated virus-CFTR gene vector in adult CF patients with mild lung disease. Hum. Gene Ther. 7, 1145–1159.

Goudy, K., Song, S., Wasserfall, C., *et al*. (2001). Adeno-associated virus vector-mediated IL-10 gene delivery prevents type 1 diabetes in NOD mice. Proc. Natl. Acad. Sci. U.S.A. 98, 13913–13918.

Griffey, M., Macauley, S.L., Ogilvie, J.M., and Sands, M.S. (2005). AAV2-mediated ocular gene therapy for infantile neuronal ceroid lipofuscinosis. Mol. Ther. 12, 413–421.

Hacein-Bey-Abina, S., Von Kalle, C., Schmidt, M., *et al*. (2003). LMO2-associated clonal T cell proliferation in two patients after gene therapy for SCID-X1. Science 302, 415–419.

Hershfield, M. (2003). Genotype is an important determinant of phenotype in adenosine deaminase deficiency. Curr. Opin. Immunol. 15, 571–577.

Hershfield, M.S., Buckley, R.H., Greenberg, M.L., *et al*. (1987). Treatment of adenosine deaminase deficiency with polyethylene glycol-modified adenosine deaminase. N. Engl. J. Med. 316, 589–596.

Inagaki, K., Fuess, S., Storm, T.A., *et al*. (2006). Robust systemic transduction with AAV9 vectors in mice: Efficient global cardiac gene transfer superior to that of AAV8. Mol. Ther. 14, 45–53.

Kapturczak, M.H., Chen, S., and Agarwal, A. (2005). Adeno-associated virus vector-mediated gene delivery to the vasculature and kidney. Acta Biochim. Pol. 52, 293–299.

Kay, M.A., Manno, C.S., Ragni, M.V., *et al*. (2000). Evidence for gene transfer and expression of factor IX in haemophilia B patients treated with an AAV vector. Nat. Genet. 24, 257–261.

Kessler, P.D., Podsakoff, G.M., Chen, X., *et al*. (1996). Gene delivery to skeletal muscle results in sustained expression and systemic delivery of a therapeutic protein. Proc. Natl. Acad. Sci. U.S.A. 93, 14082–14087.

Kohn, D.B., Sadelain, M., and Glorioso, J.C. (2003). Occurrence of leukaemia following gene therapy of X-linked SCID. Nat. Rev. Cancer 3, 477–488.

Lainka, E., Hershfield, M.S., Santisteban, I., *et al*. (2005). Polyethylene glycol-conjugated adenosine deaminase (ADA) therapy provides temporary immune reconstitution to a child with delayed-onset ADA deficiency. Clin. Diagn. Lab. Immunol. 12, 861–866.

Lipkowitz, M.S., Hanss, B., Tulchin, N., *et al*. (1999). Transduction of renal cells in vitro and in vivo by adeno-associated virus gene therapy vectors. J. Am. Soc. Nephrol. 10, 1908–1915.

Liu, T.H., Oscherwitz, J., Schnepp, B., *et al*. (2009). Genetic vaccines for anthrax based on recombinant adeno-associated virus vectors. Mol. Ther. 17, 373–379.

Lu, Y., Choi, Y.K., Campbell-Thompson, M., *et al*. (2006). Therapeutic level of functional human alpha 1 antitrypsin (hAAT) secreted from murine muscle transduced by adeno-associated virus (rAAV1) vector. J. Gene Med. 8, 730–735.

Maguire, A.M., Simonelli, F., Pierce, E.A., *et al*. (2008). Safety and efficacy of gene transfer for Leber's congenital amaurosis. N. Engl. J. Med. 358, 2240–2248.

Manno, C.S., Chew, A.J., Hutchison, S., *et al*. (2003). AAV-mediated factor IX gene transfer to skeletal muscle in patients with severe hemophilia B. Blood 101, 2963–2972.

Marshall, E. (2001). Gene therapy. Viral vectors still pack surprises. Science 294, 1640.

McCown, T.J., Xiao, X., Li, J., *et al*. (1996). Differential and persistent expression patterns of CNS gene transfer by an adeno-associated virus (AAV) vector. Brain Res. 713, 99–107.

Miyagi, N., Rao, V.P., Ricci, D., *et al*. (2008). Efficient and durable gene transfer to transplanted heart using adeno-associated virus 9 vector. J. Heart Lung Transplant. 27, 554–560.

Muzyczka, N. (1992). Use of adeno-associated virus as a general transduction vector for mammalian cells. Curr. Top. Microbiol. Immunol. 158, 97–129.

Pacak, C.A., Mah, C.S., Thattaliyath, B.D., *et al*. (2006). Recombinant adeno-associated virus serotype 9 leads to preferential cardiac transduction in vivo. Circ. Res. 99, e3–e9.

Pike-Overzet, K., van der Burg, M., Wagemaker, G., *et al*. (2007). New insights and unresolved issues regarding insertional mutagenesis in X-linked SCID gene therapy. Mol. Ther. 15, 1910–1916.

Poirier, A., Campbell-Thompson, M., Tang, Q., *et al*. (2004). Toxicology and biodistribution studies of a recombinant adeno-associated virus 2-alpha-1 antitrypsin vector. Preclinica 2, 43–51.

Snyder, R.O., and Francis, J. (2005). Adeno-associated viral vectors for clinical gene transfer studies. Curr. Gene Ther. 5, 311–321.

Song, S., Lu, Y., Choi, Y.K., *et al*. (2004). DNA-dependent PK inhibits adeno-associated virus DNA integration. Proc. Natl. Acad. Sci. U.S.A. 101, 2112-6.

Song, S., Scott-Jorgensen, M., Wang, J., *et al*. (2002). Intramuscular administration of recombinant adeno-associated virus 2 alpha-1 antitrypsin (rAAV-SERPINA1) vectors in a nonhuman primate model: Safety and immunologic aspects. Mol. Ther. 6, 329–335.

Stone, D., Liu, Y., Li, Z.Y., *et al*. (2008). Biodistribution and safety profile of recombinant adeno-associated virus serotype 6 vectors following intravenous delivery. J. Virol. 82, 7711–7715.

Toromanoff, A., Cherel, Y., Guilbaud, M., *et al*. (2008). Safety and efficacy of regional intravenous (r.i.) versus intramuscular (i.m.) delivery of rAAV1 and rAAV8 to nonhuman primate skeletal muscle. Mol. Ther. 16, 1291–1299.

Vandendriessche, T., Thorrez, L., Acosta-Sanchez, A., *et al*. (2007). Efficacy and safety of adeno-associated viral vectors based on serotype 8 and 9 vs. lentiviral vectors for hemophilia B gene therapy. J. Thromb. Haemost. 5, 16–24.

Wagner, J.A., Nepomuceno, I.B., Messner, A.H., *et al*. (2002). A phase II, double-blind, randomized, placebo-controlled clinical trial of tgAAVCF using maxillary sinus delivery in patients with cystic fibrosis with antrostomies. Hum. Gene Ther. 13, 1349–1359.

Yan, H., Guo, Y., Zhang, P., *et al*. (2005). Superior neovascularization and muscle regeneration in ischemic skeletal muscles following VEGF gene transfer by rAAV1 pseudotyped vectors. Biochem. Biophys. Res. Commun. 336, 287–298.

Address correspondence to:
Dr. Terence R. Flotte
Department of Pediatrics
University of Massachusetts Medical School
55 Lake Avenue North
Worcester, MA 01655

E-mail: Terry.Flotte@umassmed.edu

Received for publication June 14, 2010;
accepted after revision December 12, 2010.

Published online: December 13, 2010.